Synthesis and antiproliferative activity of 8-hydroxyquinoline derivatives containing a 1,2,3-triazole moiety

ARTICLE *in* EUROPEAN JOURNAL OF MEDICINAL CHEMISTRY · SEPTEMBER 2014

Impact Factor: 3.45 · DOI: 10.1016/j.ejmech.2014.07.061

European Journal of Medicinal Chemistry 84 (2014) 595–604

Contents lists available at ScienceDirect

European Journal of Medicinal Chemistry

journal homepage: http://www.elsevier.com/locate/ejmech

Original article

Synthesis and antiproliferative activity of 8-hydroxyquinoline derivatives containing a 1,2,3-triazole moiety

Luiza B. de O. Freitas [a], Thiago F. Borgati [a], Rossimiriam P. de Freitas [a], Ana L.T.G. Ruiz [b], Gabriela M. Marchetti [b], João E. de Carvalho [b], Elaine F.F. da Cunha [c], Teodorico C. Ramalho [c], Rosemeire B. Alves [a, *]

[a] Laboratório de Síntese Orgânica (Labsinto), Departamento de Química, Universidade Federal de Minas Gerais, Belo Horizonte, MG 31270-901, Brazil
[b] Divisão de Farmacologia e Toxicologia, Centro Pluridisciplinar de Pesquisas Químicas, Biológicas e Agrícolas (CPQBA), Universidade Estadual de Campinas, Campinas, CP 6171, SP 13083-970, Brazil
[c] Laboratório de Química Computacional, Departamento de Química, Universidade Federal de Lavras, CP 3037, Lavras, MG 37200-000, Brazil

ARTICLE INFO

Article history:
Received 14 February 2014
Received in revised form
16 July 2014
Accepted 19 July 2014
Available online 19 July 2014

Keywords:
8-Hydroxyquinoline
1,2,3-Triazole
"Click" reaction
Antiproliferative

ABSTRACT

Twelve novel 8-hydroxyquinoline derivatives were synthesized with good yields by performing copper-catalyzed Huisgen 1,3-dipolar cycloaddition ("click" reaction) between an 8-*O*-alkylated-quinoline containing a terminal alkyne and various aromatic or protected sugar azides. These compounds were evaluated *in vitro* for their antiproliferative activity on various cancer cell types. Protected sugar derivative **16** was the most active compound in the series, exhibiting potent antiproliferative activity and high selectivity toward ovarian cancer cells (OVCAR-03, $GI_{50} < 0.25$ μg mL^{-1}); this derivative was more active than the reference drug doxorubicin (OVCAR-03, $GI_{50} = 0.43$ μg mL^{-1}). In structure–activity relationship (SAR) studies, the physico-chemical parameters of the compounds were evaluated and docking calculations were performed for the α-glucosidase active site to predict the possible mechanism of action of this series of compounds.

1. Introduction

Cancer is an important public health concern and a significant cause of death in the human population [1]. Despite many efforts to fight cancer, the successful treatment of certain tumor types continues to be a challenge owing to their aggressiveness, the mechanisms of malignant cell metastasis, chemoresistance, and the lack of selectivity of some drugs [2]. Therefore, the development of novel anticancer agents that are safer and more effective by synthesizing small and simple molecules is necessary.

N-Heterocyclic compounds are very important in drug design [3–5]. Among these, quinoline and its derivatives are present in several classes of natural and synthetic biologically active compounds [6–8]. In particular, 8-hydroxyquinoline and its derivatives are of interest because of their wide spectrum of biological activities such as cytotoxic [9–11], antifungal [12–14], antibacterial [13–15], antifilarial [16], and HIV integrase inhibitory [17] activities.

Triazoles, another important class of *N*-heterocycles, are employed in many pharmaceutical products. In particular, 1,2,3-triazoles are of great relevance to medicinal chemistry because they can act as pharmacophores and linkers between two or more substances of interest in molecular hybridization approaches [18]. In recent years, 1,2,3-triazoles have gained special attention in the drug discovery field because of the growing use of copper-catalyzed azide-alkyne cycloaddition—the "click" reaction [19,20]. Compounds containing a 1,2,3-triazole display a wide range of biological activities such as cytotoxic [2,21–23], antibacterial [6,24,25], antifungal [6,26,27], antimalarial [28], and trypanocidal [29,30] activities.

A series of quinoline derivatives carrying additional aromatic rings—derivatives **1** [11], **2** [31] and **3** [10]—have been reported to possess potential anticancer activities (Fig. 1). Notably, these compounds often contain halogen substituents. In some instances, sugar moieties have been used to improve the solubility of compounds or to act as key molecular recognition and communication elements [10,32].

By considering the possibility of building a single molecular framework containing two or more heterocycles of promising biological activity, we aimed to synthesize a series of compounds

* Corresponding author.
E-mail addresses: rosebrondi@yahoo.com.br, lubofbof@gmail.com (R.B. Alves).

http://dx.doi.org/10.1016/j.ejmech.2014.07.061
0223-5234/

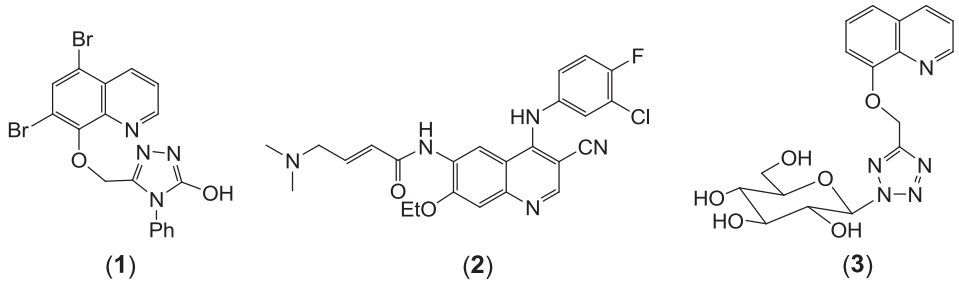

Fig. 1. Representative examples of biologically active quinoline derivatives.

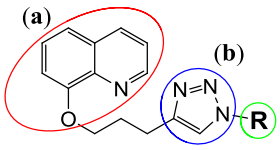

Fig. 2. General structures of the synthesized quinoline derivatives carrying a 1,2,3-triazole moiety.

comprising an 8-*O*-alkylated-quinoline (**a**), a 1,2,3-triazole nucleus (**b**), and an aromatic or sugar moiety (**R**) (Fig. 2). We chose aromatic rings bearing different halogen substituents (F, Cl, Br, and I) or sugar derivatives to evaluate the electronic and steric influences of these substituents on the activities of the derivatives. Derivatization of the hydroxyl group from 8-hydroxyquinoline by attaching a 1,2,3-triazole has not been used previously for the purpose of evaluating the biological activities of its derivatives [33,34]. The *in vitro* antiproliferative activity of these new compounds was investigated on various cancer cell types and some structure–activity relationship (SAR) studies were conducted.

2. Results and discussion

2.1. Chemistry

In our approach for the synthesis of 8-hydroxyquinoline derivatives, we developed a synthetic route that used the click reaction to couple 8-*O*-alkylated-quinoline containing terminal alkyne moiety **7** to benzyl azide derivatives **9a**–**i** in the presence of a Cu(I) catalyst (Scheme 1).

The required starting material, 8-*O*-alkylated-quinoline containing a terminal alkyne moiety (**7**), was obtained in a good yield (88%) by performing etherification of 8-hydroxyquinoline with 4-pentyn-1-ol methanesulfonate under phase-transfer catalysis using tetrabutylammonium bromide (TBAB). 4-Pentyn-1-ol methanesulfonate was prepared according to a previously described method [35]. To prepare benzyl azides **9a**–**i**, the corresponding benzyl alcohols **a**–**i** were mesylated. Nucleophilic substitution reactions of resultant mesylates **8a**–**i** were then performed using sodium azide in dimethyl sulfoxide (DMSO) at room temperature. Benzyl azides **9a**–**i** were obtained in high yields (72–99%). To obtain the 1,2,3-triazoles, solutions of alkyne **7** with each benzyl azide derivative (**9a**–**i**) in dichloromethane were treated with a solution of copper sulfate pentahydrate (8 mol%) and sodium ascorbate (20 mol%) in water. The reaction mixtures were stirred for 2 h, at room temperature, to exclusively obtain 1,4-disubstituted 1,2,3-triazoles **10a**–**i** with good yields (67–94%).

We also synthesized three new analogs (**15**, **16**, and **17**) belonging to this family of compounds, based on the 8-*O*-alkylated-quinoline scaffold that contained a triazole. We added substituents predicted to increase biological activity, such as a pyridine nucleus [2], protected sugar group [36], or an ester group (Scheme 2) [22].

As shown in Scheme 2, 3-pyridinepropanol was first brominated using HBr under microwave irradiation. The brominated compound

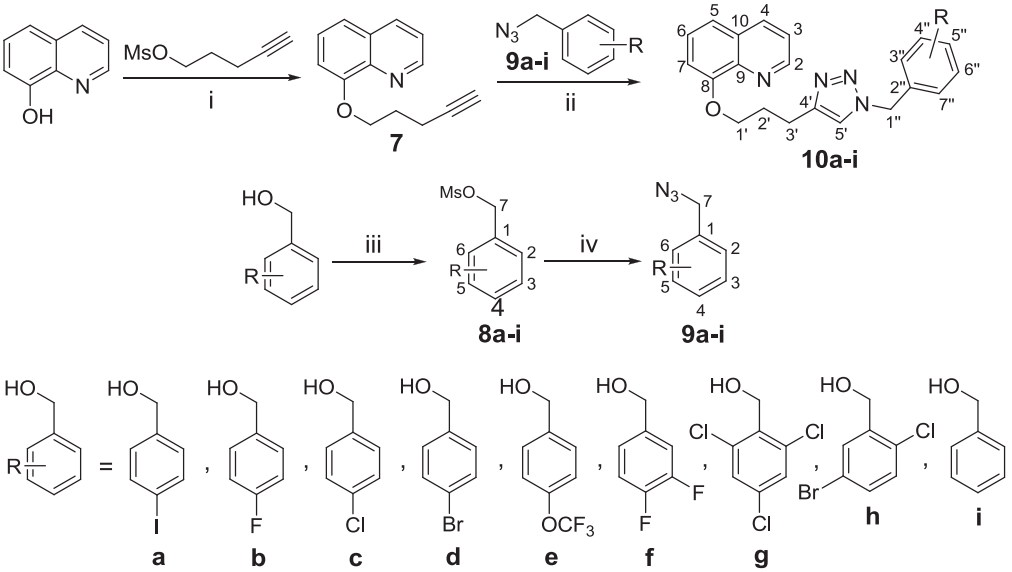

Scheme 1. Reagents and conditions: (i) TBAB, NaOH (50% w/v), Et_2O/H_2O, r.t., 48 h; (ii) NaAsc (20 mol%), $CuSO_4 \cdot 5H_2O$ (8 mol%), CH_2Cl_2/H_2O (1:1), r.t., 2 h; (iii) MsCl, Et_3N, CH_2Cl_2, −40 °C, 30 min; (iv) NaN_3, DMSO, r.t., 15 h.

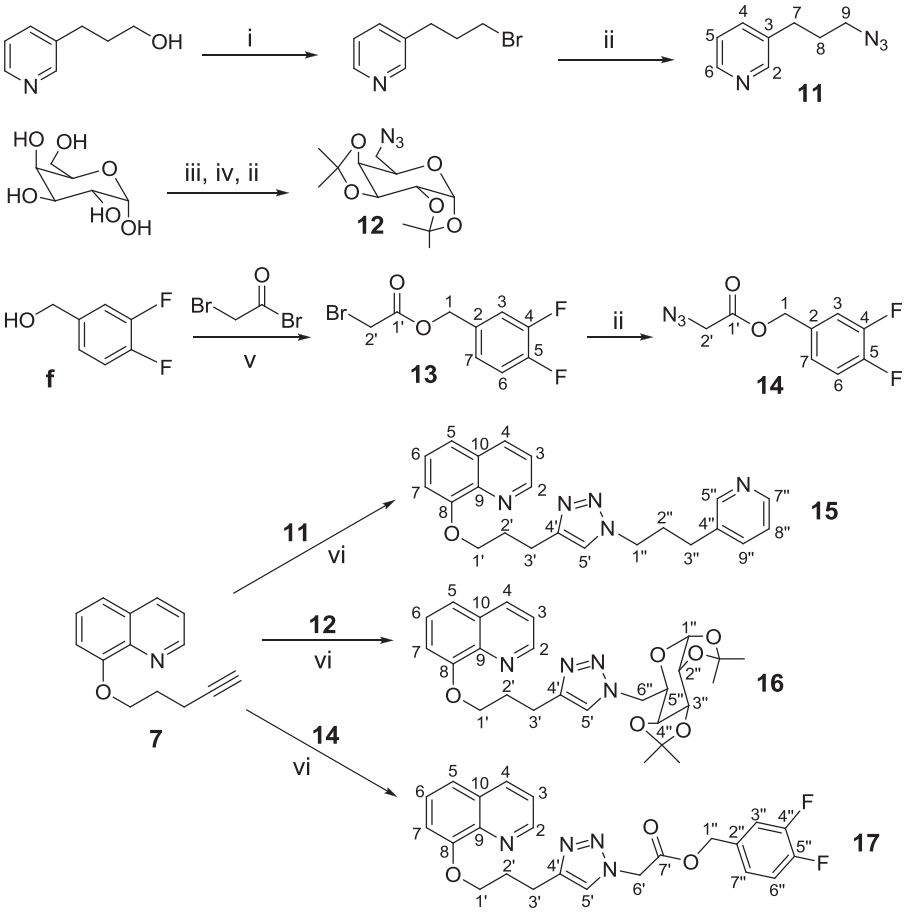

Scheme 2. Reagents and conditions: (i) HBr, microwave, 200 W, 11 min, 80 °C; (ii) NaN_3, DMSO, r.t., 24 h; (iii) acetone, $CuSO_4$, H_2SO_4, r.t., 24 h; (iv) MsCl, Et_3N, CH_2Cl_2, −40 °C, 30 min; (v) Et_3N, DMAP, CH_2Cl_2, 0 °C − r.t. (vi) NaAsc (20 mol%), $CuSO_4 \cdot 5H_2O$ (8 mol%), CH_2Cl_2/H_2O (1:1), r.t., 2 h.

was converted to 3-(3-azidopropyl)pyridine **11** by performing nucleophilic substitution using sodium azide in DMSO at room temperature. A three-step protocol was used to obtain 1,2:3,4-di-*O*-isopropylidene-6-azido-α-D-galactopyranose **12** from D-galactose, as previously reported [36]. Azido ester **14** was obtained in two steps. First, benzyl alcohol derivative **f** and bromoacetyl bromide were reacted in dichloromethane containing 4-dimethylaminopyridine (DMAP) and triethylamine to generate bromo ester **13**. Next, bromo ester **13** was subjected to nucleophilic substitution by using sodium azide in DMSO at room temperature to obtain azido ester **14**. Finally, the 1,2,3-triazole derivatives **15**, **16**, and **17** were obtained from **11**, **12**, and **14**, respectively, by using the same click reaction methodology that was applied to obtain compounds **10a**–**i**.

2.2. Antiproliferative studies

The antiproliferative activity of the tested compounds were expressed as the concentration that produced 50% cell growth

Table 1
Antiproliferative activity (GI_{50} in μg mL^{-1}) and MG MID (Log GI_{50}) of synthesized compounds against selected human cell lines.

Compounds	Cell lines								MG MID log GI_{50}
	U251	MCF-7	NCI-ADR/RES	786-0	NCI-H460	PC-3	OVCAR-03	HaCat	
DOX	0.039	0.038	0.54	0.15	<0.025	3.8	0.43	0.11	−0.8
10a	>250	25.0	>250	22.6	24.6	24.7	24.7	>250	1.8
10b	20.7	11.7	49.4	195.1	34.4	20.1	23.1	115.1	1.6
10c	3.4	6.2	11.6	2.8	11.2	3.6	8.1	4.2	0.7
10d	8.4	28.0	25.8	25.9	11.7	8.4	27.2	29.2	1.3
10e	9.8	3.1	5.5	7.9	10.4	5.0	24.5	4.0	0.9
10f	18.2	21.3	42.1	8.5	23.7	6.6	63.5	41.7	1.3
10g	3.1	2.9	2.8	5.6	7.4	2.8	11.4	5.3	0.7
10h	8.7	9.6	2.5	>250	7.9	8.2	8.0	4.9	1.0
10i	25.2	12.7	10.4	25.0	28.6	16.8	24.3	12.7	1.3
15	25.1	27.8	12.5	69.4	44.3	26.7	39.1	25	1.5
16	24.3	2.6	28.6	30.8	30.1	16.2	<0.25	29.4	1.0
17	26.5	27.2	4.9	26.1	29.2	2.9	15.1	21.4	1.2

GI_{50}, Growth Inhibition 50%; MG MID, mean graph midpoint; DOX, doxorubicin. Human cancer cell lines: U251 (glioma, central nervous system), MCF-7 (breast), NCI-ADR/RES (ovarian, multidrug resistant), 786-0 (kidney), NCI-H460 (lung, non-small cell), PC-3 (prostate), and OVCAR-03 (ovarian). Normal cell line: HaCat (human keratinocytes).

inhibition or a cytostatic effect (GI_{50}, μg mL^{-1}) for each cell line (Table 1). Almost all of the compounds tested inhibited cell growth in a dose-dependent manner (Supplementary data S1). A mean graph midpoint (MG MID, mean of log GI_{50}) value was also calculated for each compound. Among the synthesized 1,2,3-triazoles, the best results were obtained for derivatives **10c**, **10g**, **10e**, **10h**, and **16**, each of which had MG MID GI_{50} values less than or equal to 1.0 (Table 1). Derivative **10c** was as effective against PC-3 cells as doxorubicin (**10c** GI_{50} = 3.6 μg mL^{-1}; doxorubicin GI_{50} = 3.8 μg mL^{-1}). Derivative **10h** showed the best inhibitory effect against the NCI-ADR/RES cancer cell line (GI_{50} = 2.5 μg mL^{-1}). Protected sugar derivative **16** had the lowest GI_{50} value against OVCAR-03 cells (GI_{50} < 0.25 μg mL^{-1}), indicating that it was even more active than doxorubicin (OVCAR-03, GI_{50} = 0.43 μg mL^{-1}). Although derivative **16** had high selectivity for ovarian cancer cell lines, it showed weak antiproliferative activity against other cancer cell lines and HaCat cells.

Given that **10c** and **10g** had the best MG MID log GI_{50} values among the halogenated derivatives, these results suggested that chlorinated substituents afforded better cytostatic activity. Moreover, the presence of one or three chlorine substituents resulted in almost the same cytostatic effect (**10c** and **10 g** MG MID GI_{50} = 0.7). The addition of an ester group between the triazole ring and benzyl derivative (compound **17**) improved the antiproliferative activity against some cell lines (PC-3, NCI-ADR/RES, and OVCAR-3), because it contributed to an increase in cytotoxic activity when compared to **10f**. However, compounds **10f** and **17**, both showed weak cytotoxic effects on average (**10f** MG MID GI_{50} = 1.3; **17** MG MID GI_{50} = 1.2). The antiproliferative activity of compounds **10g** and **17** against prostate cell lines (PC-3, **10g**GI_{50} = 2.8 μg mL^{-1}; **17** GI_{50} = 2.9 μg mL^{-1}) was slightly better than that of doxorubicin (PC-3, GI_{50} = 3.8 μg mL^{-1}). Other derivatives, such as those containing bromide (**10d**, MG MID GI_{50} = 1.3), a benzyl group (**10i**, MG MID GI_{50} = 1.3), pyridine (**15**, MG MID GI_{50} = 1.5), fluorine (**10b**, MG MID GI_{50} = 1.6), or iodine (**10a**, MG MID GI_{50} = 1.8), did not exhibit significant activity.

The selectivity index (SI) was calculated for each compound (Table 2). Derivative **16** showed the highest SI value, which indicated the potential use of this compound for future *in vivo* tests.

To reach their target sites, bioactive compounds have to cross several barriers. Their bioavailability depends upon several parameters such as solubility, membrane permeability, as well as active uptake and transport within the organism [37]. Lipinski and colleagues defined the properties and molecular features that are associated with orally active drugs in humans and summarized them in the "rule-of-five" [38]. Veber and co-workers later added additional related criteria [39]. These parameters have been widely used as a filter for new potential drugs. Therefore, a computational study was performed to predict the physico-chemical parameters of the synthesized compounds to verify if the substances could fulfill Lipinski's rule-of-five (Tables 3 and 4). These parameters were calculated using Molinspiration, free software that can be used to predict properties of compounds [40]. The hydrogen-bonding capacity—the number of hydrogen bond acceptors (HBA)—was estimated based on the number of nitrogen and oxygen atoms in the chemical structure. The number of hydrogen bond donors (HBD) corresponds to the sum of hydrogen atoms bound to oxygen or nitrogen atoms [38,41]. The polar surface area (PSA) was also calculated because it is another important property that has been used to predict drug bioavailability. Passively absorbed molecules with PSA values >140 are thought to have low oral bioavailability [42]. The violation of more than one of these rules may indicate problems in the bioavailability of a potential drug.

The results (Table 4) showed that all the compounds complied with Lipinski's rules (Table 3), with the exception of compounds **10g** and **10h**, which had calculated lipophilicity (c*Log*P) values slightly higher than what is ideal for orally active drugs (≤5), and compound **16**, which had one additional rotatable bond (nRotB) than what is ideal. Theoretically, compounds **10a**–**f**, **10i**, **15**, and **17** should show good passive absorption and, thus, their differences in bioactivity cannot be attributed to this property [43].

Using structure–activity relationship (SAR) studies, physical–chemical parameters were calculated for each compound. Multiple linear regression was used to model the relationship between the independent electronic and physicochemical descriptors and GI_{50} values by fitting a linear equation to the observed data. The calculated GI_{50} values were obtained using the following equation:

$$pIG_{50} = \sum_{i=1}^{N} C_i P_i \quad (1)$$

Table 2
Selective index (SI) for each synthesized compound.

Compounds	Cell lines						
	U251	MCF-7	NCI-ADR/RES	786-0	NCI-H460	PC-3	OVCAR-03
10a	–	>10.0	–	>11.1	>10.2	>10.1	>10.1
10b	5.6	9.8	2.3	0.6	3.3	5.7	5.0
10c	1.2	0.7	0.4	1.5	0.4	1.2	0.5
10d	3.5	1.0	1.1	1.1	2.5	3.5	1.1
10e	0.4	1.3	0.7	0.5	0.4	0.8	0.2
10f	2.3	1.9	1.0	4.9	1.8	6.3	0.7
10g	1.7	1.8	1.9	0.9	0.7	1.9	0.5
10h	0.6	0.5	2.0	–	0.6	0.6	0.6
10i	0.5	1.0	1.2	0.5	0.4	0.8	0.5
15	1.0	0.9	2.0	0.4	0.6	0.9	0.6
16	1.2	11.3	1.0	0.9	1.0	1.8	>117.6
17	0.8	0.8	4.4	0.8	0.7	7.4	1.4

Human cell lines: U251 (glioma, CNS), MCF-7 (breast), NCI-ADR/RES (ovarian expressing phenotype multiple drugs resistance), 786-0 (kidney), NCI-H460 (lung, non-small cells), PC-3 (prostate) and OVCAR-03 (ovarian).

Table 3
Reference values of the rules of Lipinski and Veber.

Comp.	cLogP	MW	PSA	HBD	HBA	nRotB
Lipinski[a]	≤5	≤500	–	≤5	≤10	–
Veber[b]	–	–	≤140			≤10

[a] Lipinski's Rule of 5 for pharmaceuticals.
[b] Veber added more criteria to Lipinski's Rule of 5.

Table 4
Predicted physicochemical properties of compounds **10a**–**i**, **15**, **16** and **17**.

Comp.	cLogP	MW	PSA	HBD	HBA	nRotB
10a	4.79	470.3	49.55	0	5	7
10b	3.81	362.4	49.55	0	6	7
10c	4.37	378.9	49.55	0	5	7
10d	4.53	423.3	49.55	0	5	7
10e	4.70	428.4	58.78	0	9	9
10f	3.88	380.4	49.55	0	7	7
10g	5.80	447.7	49.55	0	5	7
10h	5.24	457.8	49.55	0	5	7
10i	3.67	344.4	49.55	0	5	7
15	4.37	372.5	49.55	0	5	9
16	2.94	496.6	95.70	0	10	11
17	3.92	438.4	75.85	0	9	10

cLogP: calculated lipophilicity; MW: molecular weight; PSA: polar surface area; HBD: number of hydrogen bond donor; HBA: number of hydrogen bond acceptor; nRotB: number of rotatable bounds.

where *Ci* is the coefficient obtained from the multivariable regression and *Pi* is a physicochemical property.

We have used cell lines for which experimental data have been defined for all the studied compounds. Thus, the theoretical model proposal included the same compounds for comparison. Based on this criterion, cell lines MCF-7 and PC-3 were selected. For the MCF-7 cancer cell line, the following equation was obtained using an R^2 value of 0.42:

$$\begin{aligned} GI_{50} = {} & -0.036(\text{dipole}) + 52.093(\text{HOMO}) + 42.457(\text{HOMO}-1) \\ & + 3.799(\text{HOMO}-2) - 25.855(\text{HOMO}-3) \\ & - 34.067(\text{LUMO}) - 0.002(\text{Log P}) + 19.020 \end{aligned} \quad (2)$$

The R^2 value suggested a poor correlation between biological activity and physicochemical descriptors. Therefore, those descriptors are not sufficient to explain the antiproliferative activity against the MCF-7 cell line. However, for the PC-3 cell line, an R^2 greater than 0.7 ($R^2 = 0.86$) was determined for the data [44], indicating a high correlation. This suggested that antiproliferative activity was linked to some electronic/physicochemical properties. Equation (3) was established for all the studied compounds (Table 1).

$$\begin{aligned} GI_{50} = {} & -0.153(\text{dipole}) + 124.604(\text{HOMO}) \\ & - 108.748(\text{HOMO}-1) + 39.584(\text{HOMO}-2) \\ & - 22.526(\text{HOMO}-3) - 133.758(\text{LUMO}) \\ & - 0.217(\text{Log P}) + 6.120 \end{aligned} \quad (3)$$

It should be kept in mind that negative values represent higher antiproliferative activity values. The frontier molecular orbitals—highest occupied and lowest unoccupied molecular orbitals (HOMO and LUMO, respectively)—greatly affected the potency of the compounds (Eq. (3)). Thus, positive coefficients corresponded to unfavorable biological activity values. In order words, these properties decreased the potencies of the studied compounds. We have calculated the HOMO and LUMO energy values in order to investigate the effect of electronic parameters on the antiproliferative activity of each compound. The HOMO has the priority to provide electrons, while the LUMO is the first to accept electrons. According to the frontier molecular orbital theory, the HOMO and LUMO are two important factors that affect the bioactivity of compounds. A small difference between the HOMO and LUMO energy values implies high reactivity in reactions, while a large difference implies low reactivity [45]. In addition to the energy difference between the HOMO and LUMO, the individual positions of these orbitals affected the reactivity of the compounds. Fig. 3 shows the molecular orbitals for compound **10g**, which showed antiproliferative activity that was more potent than the reference drug doxorubicin (PC-3, $GI_{50} = 3.8\ \mu g\ mL^{-1}$).

Although the SAR results appeared to be promising, a deeper understanding of these results required the application of other molecular modeling techniques such as docking calculations. Recently, Chinthala and co-workers [46] showed the association between α-glucosidase inhibition and the anticancer activity profiles of 1,2,3-triazoles derivatives towards human cancer cell lines. In fact, glycosidase inhibitors have been studied in the field of cancer research as agents that are able to inhibit tumor cell invasion and migration [47,48].

To gain further insight into the bioactivity of the compounds and SAR results, we investigated the binding mode of 8-hydroxyquinoline derivatives to α-glucosidase by performing docking calculations. Fig. 4 shows the interaction mode between compound **10g** and α-glucosidase. Compound **10g** was found to be more active than any other inhibitor. This result is in agreement with the antiproliferative activity reported in Table 1. In fact, compound **10g** was found to hydrogen bond to Arg643 and Arg647 of α-glucosidase, and its benzyl group participated in an anion-π interaction with α-glucosidase Glu767, as illustrated in Fig. 4.

In addition to the orbital energy values and hydrogen bond information determined using docking calculations, HOMO–LUMO three-dimensional structures were also examined. The obtained data showed that the HOMO structures of all the compounds were located in the quinoline ring and, notably, the LUMO was located on the triazole ring and benzyl group (Fig. 3). These data were expected because the HOMO was in the electron-rich portion, whereas the LUMO was in electron-poor region. Therefore, it is worth mentioning that the HOMO structure was located in the same region in all of the compounds and showed a good correlation for the cell line PC-3. This feature clearly showed a preference for specific reaction sites. Our docking findings showed that the triazole ring and benzyl group were oriented inside the active site and interacted strongly with Arg647 and Glu767. Thus, the LUMO structure of the inhibitor was directed to those amino acid residues, while the quinoline ring was oriented to the protein surface. These results suggest that the conformational preference of 8-hydroxyquinoline derivatives containing 1,2,3-triazole moieties is attributable to the interaction between the LUMO (from the inhibitor) and HOMO (from α-glucosidase Glu767).

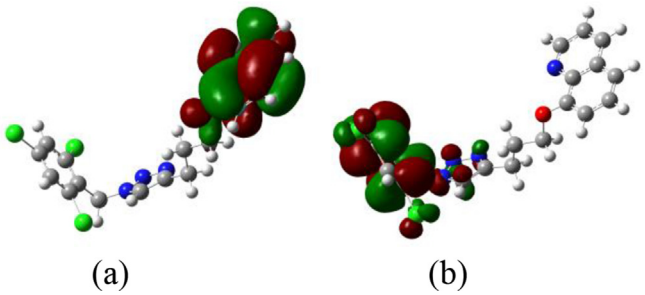

Fig. 3. Molecular orbital surfaces of compound **10g**. (a) The highest occupied molecular orbital and (b) lowest unoccupied molecular orbital.

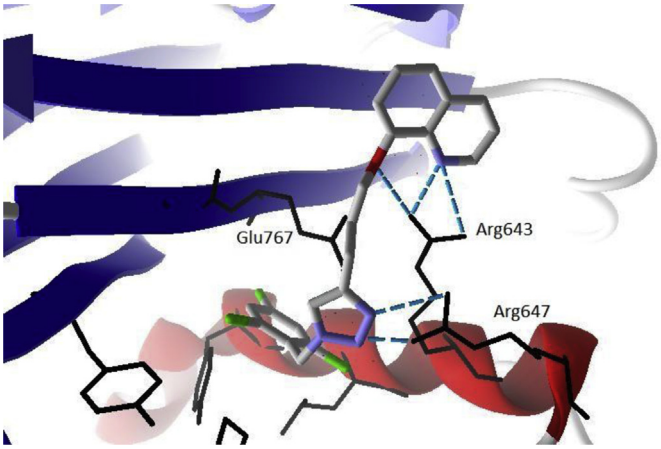

Fig. 4. Docked structure of compound **10g** in the α-glucosidase active site. The residues shown are those involved in hydrogen bonding with the inhibitor.

3. Conclusions

We have synthesized 12 novel 8-hydroxyquinoline derivatives in good yields by using the click reaction, coupling an 8-*O*-alkylated-quinoline containing a terminal alkyne with an aromatic group or protected sugar azide. In general, the compounds showed favorable physico-chemical parameters that qualify these compounds to be explored as anticancer agents. These molecules were evaluated *in vitro* for their antiproliferative activity on various cancer cell types. Among the halogenated derivatives, the chlorinated ones showed the best overall activity, with **10c** and **10g** both showing the lowest MG MID GI_{50} value of 0.7. Our findings also suggest the importance of the location of the frontier orbitals (HOMO and LUMO) in the studied compounds for their activity toward prostate cancer cells. The HOMO of all compounds is located on the quinoline, while the LUMO is located on the triazole ring and benzyl group (Fig. 3). Our docking calculation data reinforce that the binding orientation of the inhibitors in the active site of α-glucosidase is likely governed by the interaction between the HOMO and LUMO orbitals. Additional accurate theoretical calculations and experimental techniques are now in progress in order to garner a deeper understanding of the antiproliferative activity of this series of compounds. Protected sugar derivative **16** was the most active against and highly selective for ovarian cancer cells (OVCAR-03, $GI_{50} < 0.25$ μg mL^{-1}), showing greater activity against these cells than doxorubicin (OVCAR-03, $GI_{50} = 0.43$ μg mL^{-1}). The high antiproliferative activity and selectivity of compound **16** has driven efforts to synthesize other analogs containing sugar moieties that can be further studied with respect to their anticancer activity and mechanisms of action.

4. Materials and methods

4.1. Reagents and equipment

Commercially available reagents were purchased from Sigma–Aldrich and used without further purification. The solvents were purified by distillation. The melting points were determined on a Büchi apparatus and were uncorrected. Column chromatography was performed on Silica Gel 60 (70–230 mesh, Merck). The progress of the reactions was monitored by thin-layer chromatography using Merck silica plates (GF_{254}). ^1H and ^{13}C NMR spectra were recorded using a Bruker AVANCE DRX 200 MHz or 400 MHz spectrometer by using tetramethylsilane as an internal standard. The results are presented as the chemical shift δ in ppm, number of protons, multiplicity, *J* values in Hertz, proton position, and carbon position. Multiplicities are abbreviated as follows: s, singlet; brs, broad signal; d, doublet; dd, double doublet; t, triplet; m, multiplet; qn, quintet; and td, triple doublet. Infrared spectra were recorded on a Perkin–Elmer Spectrum One SP-IR Spectrometer. The microwave reactor used was a CEM Discover. High-resolution mass spectra were recorded using an LC-MS Bruker Daltonics Micro electrospray ionization-time-of-flight mass spectrometer (solvent: MeOH/H_2O, 1:1).

4.2. Synthesis

4.2.1. Synthesis of 8-(pent-4-ynyloxy)quinoline (**7**)

Diethyl ether (12 mL), 8-hydroxyquinoline (2.76 mmol), 4-pentyn-1-ol methanesulfonate (3.30 mmol), and TBAB (0.82 mmol) were added to a 50-mL round-bottom flask. To this solution, 10 mL of an aqueous 50% NaOH (w/v) solution was added. The reaction mixture was stirred for 48 h at room temperature. After 48 h, 30 mL of water was added to the reaction mixture, followed by extraction with dichloromethane (3 × 25 mL). The combined organic phases were dried over anhydrous sodium sulfate and removed by performing distillation. The remaining residue was purified by column chromatography on silica gel using hexane:ethyl acetate (7:3) to produce pure compound **7**.

Pale-yellow crystals; yield 88%; m.p. 69–71 °C; IR (ATR): 3174 (≡C–H), 2106 (C≡C), 1262 and 1082 (C–O); ^1H NMR (200 MHz, $CDCl_3$): δ 1.99 (1H, t, $J = 2.6$ Hz, H-5′), 2.24 (2H, qn, $J = 6.6$ Hz, H-2′), 2.51 (2H, td, $J = 6.6$ and 2.6 Hz, H-3′), 4.35 (2H, t, $J = 6.6$ Hz, H-1′), 7.09 (1H, dd, $J = 7.2$ and 1.4 Hz, H-7), 7.35–7.49 (3H, m, H-3, H-5, H-6), 8.11 (1H, dd, $J = 8.4$ and 1.6 Hz, H-4), 8.95 (1H, dd, $J = 4.2$ and 1.6 Hz, H-2); ^{13}C NMR (50 MHz, $CDCl_3$): δ 15.51 (C-3′), 27.94 (C-2′), 67.39 (C-1′), 69.12 (C-5′), 83.63 (C-4′), 108.98 (C-7), 119.76 (C-5), 121.65 (C-3), 126.82 (C-6), 129.59 (C-10), 136.14 (C-4), 140.28 (C-9), 149.31 (C-2), 154.69 (C-8).

4.3. General procedure for the synthesis of benzyl mesylates (***8a–i***)

Each benzyl alcohol derivative (1.00 mmol) was combined with dichloromethane (5 mL) and triethylamine (280 μL, 2.01 mmol) in a 50-mL round-bottom flask. The mixture was cooled to −40 °C, and methanesulfonyl chloride (110 μL, 1.40 mmol) was added to the mixture while being stirred vigorously. After 30 min at −40 °C, the reaction mixture was washed with a 1% HCl solution (3 × 10 mL) and a saturated aqueous $NaHCO_3$ solution (3 × 5 mL). The organic layer was dried (Na_2SO_4), filtered and the solvent was removed *in vacuo* to produce high yields (90–100%) of pure benzyl mesylates **8a–i**.

4.3.1. 4-Iodobenzyl methanesulfonate (***8a***)

Colorless oil; yield 90%; ^1H NMR (200 MHz, $CDCl_3$): δ 2.94 (3H, s, CH_3), 5.14 (2H, s, C-7), 7.13 (2H, d, $J = 8.4$ Hz, H-2, H-6), 7.70 (2H, d, $J = 8.4$ Hz, H-3, H-5); ^{13}C NMR (50 MHz, $CDCl_3$): δ 38.23 ($\underline{C}H_3$), 70.64 (C-7), 95.38 (C-4), 130.47 (C-2, C-6), 133.13 (C-1), 137.98 (C-3 and C-5).

4.4. General procedure for the synthesis of benzyl azides (***9a–i***)

Benzyl mesylate (0.77 mmol), DMSO (5 mL), and sodium azide (0.200 g, 3.08 mmol) were added to a 50-mL round-bottom flask. The reaction mixture was stirred at room temperature for 15 h. Dichloromethane (15 mL) was then added and the resulting mixture was washed with brine (3 × 10 mL). The organic phase was dried (Na_2SO_4) and distilled. This procedure produced good yields (72–99%) of pure benzyl azides **9a–i**.

4.4.1. 1-(Azidomethyl)-4-iodobenzene (***9a***)

Colorless oil; yield 85%; IR (ATR): 2109 ($N{=}N^+{=}N^-$); ^1H NMR (200 MHz, $CDCl_3$): δ 4.29 (2H, s, H-7), 7.07 (2H, d, $J = 8.4$ Hz, H-2, H-6), 7.72 (2H, d, $J = 8.4$ Hz, H-3, H-5); ^{13}C NMR (50 MHz, $CDCl_3$): δ 54.16 (C-7), 94.08 (C-4), 130.02 (C-2, C-6), 135.07 (C-1), 137.94 (C-3, C-5).

4.4.2. Synthesis of 3-(3-azidopropyl)pyridine (***11***)

3-Pyridine-propanol (0.400 g, 2.92 mmol) and HBr 47% (w/w aq., 4 mL, 34.60 mmol) were added to a 50-mL round-bottom flask. The mixture was irradiated with microwaves for 11 min at 80 °C (200 W, atmospheric pressure). After the reaction mixture was cooled to room temperature, it was neutralized using a saturated solution of $NaHCO_3$. The resultant solution was extracted with dichloromethane (3 × 15 mL). The organic layer was dried (Na_2SO_4) and filtered, and the solvent was removed *in vacuo* to produce the crude product (3-(3-bromopropyl)pyridine), a yellow oil. The crude product was immediately subjected to nucleophilic substitution with NaN_3. A stock solution of NaN_3 (0.5 mol/L) in DMSO was prepared by stirring the solution for 24 h at 25 °C. A portion of the

NaN_3 solution (8 mL, containing 4.00 mmol of NaN_3) and 3-(3-bromopropyl)pyridine (0.525 mg, 2.62 mmol) were added to a 50-mL round-bottom flask equipped with a magnetic stir bar. The mixture was stirred for 24 h at room temperature. After the reaction was complete, 3 mL of cold water was added, and the mixture was stirred for 5 min. The reaction was then quenched using H_2O (50 mL) and stirred for an additional 5 min. Next, the mixture was extracted with dichloromethane (3 × 30 mL), and the resultant combined organic extracts were washed with H_2O (2 × 50 mL) and brine (3 × 50 mL). The organic layer was dried (Na_2SO_4) and filtered, and the solvent was removed *in vacuo* to produce pure 3-(3-azidopropyl)pyridine **11**.

Colorless oil; yield 64%; ^{1}H NMR (200 MHz, $CDCl_3$): δ 1.89 (2H, qn, J = 7.4 Hz, H-8), 2.70 (2H, t, J = 7.4 Hz, H-7), 3.30 (2H, t, J = 7.4 Hz, H-9), 7.19–7.25 (1H, m, H-5), 7.50 (1H, d, J = 7.8 Hz, H-4), 8.45 (2H, s, H-2, H-6); ^{13}C NMR (50 MHz, $CDCl_3$): δ 30.04 (C-7 or C-8), 30.26 (C-8 or C-7), 50.56 (C-9), 123.61 (C-5), 136.15 (C-3, C-4), 147.69 (C-6), 149.86 (C-2).

4.4.3. Synthesis of 3,4-difluorobenzyl 2-bromoacetate (**13**)

(3,4-Difluorophenyl)methanol (1.39 mmol), DMAP (0.139 mmol), triethylamine (195 μL, 1.39 mmol), and dichloromethane (2 mL) were combined in a 15-mL round-bottom flask. Before the addition of bromoacetyl bromide (120 μL, 1.39 mmol), the reaction mixture was cooled to 0 °C while being stirred vigorously. The mixture was maintained at 0 °C for 20 min, followed by 30 min at room temperature. Next, 5 mL of cold water was added to the reaction mixture and it was then extracted with dichloromethane (3 × 8 mL). The organic layer was dried (Na_2SO_4), filtered, and the solvent was removed *in vacuo* to produce the crude product. The crude product was purified by column chromatography on silica gel using hexane:ethyl acetate (8:2) to obtain pure compound **13**.

Pale yellow oil; yield 99%; IR (ATR): 1738 (C=O), 1277 (C–F); ^{1}H NMR (200 MHz, $CDCl_3$): δ 3.88 (2H, s, H-2′), 5.14 (2H, s, H-1), 7.11–7.27 (3H, m, H-3, H-6, H-7); ^{13}C NMR (50 MHz, $CDCl_3$): δ 25.67 (C-2′), 66.65 (C-1), 117.66 (d, J = 17.0 Hz, C-3, C-6), 124.77 (d, J = 3.5 Hz, H-7), 132.21 (d, J = 4.6 Hz, C-2), 148.10–153.17 (m, C-4, C-5), 167.06 (C-1′).

4.4.4. Synthesis of 3,4-difluorobenzyl 2-azidoacetate (**14**)

3,4-Difluorobenzyl 2-bromoacetate (**13**) (1.51 mmol), sodium azide (4.53 mmol), and DMSO (3 mL) were added to a 15-mL round-bottom flask. The reaction mixture was stirred at room temperature for 24 h. Dichloromethane (15 mL) was added and the resulting mixture was washed with brine (3 × 10 mL). The organic layer was dried (Na_2SO_4), filtered, and concentrated under reduced pressure to produce the crude product. The crude product was purified by column chromatography on silica gel using hexane:ethyl acetate (1:1) to obtain pure compound **14**.

Pale yellow oil; yield 80%; IR (ATR): 2105 (N=N$^+$=N$^-$), 1746 (C=O), 1288 (C–F); ^{1}H NMR (200 MHz, $CDCl_3$): δ 3.92 (2H, s, H-2′), 5.17 (2H, s, H-1), 7.11–7.25 (3H, m, H-3, H-6, H-7); ^{13}C NMR (50 MHz, $CDCl_3$): δ 50.37 (C-2′), 66.23 (C-1), 117.49–117.92 (m, C-3, C-6), 124.81–125,00 (m, C-7), 132.01–132.20 (m, C-2), 147.72–153.31 (m, C-4, C-5), 168.20 (C-1′).

4.5. General procedure for the synthesis of compounds (**10a–i**, **15**, **16** and **17**)

Each of the azide compounds (**9a–i**, **11**, **12**, or **14**) (1.00 equiv.) and 8-(pent-4-ynyloxy)quinoline (**7**) (1.00 equiv.) were dissolved in CH_2Cl_2. To this solution, a freshly prepared solution of $CuSO_4 \cdot 5H_2O$ (0.08 equiv.) and sodium ascorbate (0.20 equiv.) in H_2O was added while being stirred vigorously. The reaction mixture was stirred for 2 h at room temperature. After the reaction was complete, 5 mL of water was added to the reaction mixture, followed by extraction with CH_2Cl_2 (3 × 8 mL). The organic layer was dried (Na_2SO_4), filtered, and then removed under reduced pressure to produce the crude product. The crude product was purified by column chromatography on silica gel using EtOAc, and eluted using EtOAc:MeOH (9:1–8:2) to obtain pure compounds **10a–i**, **15**, **16**, and **17**.

4.5.1. 8-(3-(1-(4-Iodobenzyl)-1H-1,2,3-triazol-4-yl)propoxy) quinoline (**10a**)

Yellow-white solid; m.p. 108–109 °C; yield 86%; IR (ATR): 1108 (C–O); ^{1}H NMR (200 MHz, $CDCl_3$): δ 2.32–2.42 (2H, m, H-2′), 3.01 (2H, t, J = 7.4 Hz, H-3′), 4.28 (2H, t, J = 7.4 Hz, H-1′), 5.40 (2H, s, H-1″), 6.94 (2H, d, J = 8.3 Hz, H-3″, H-7″), 7.04 (1H, dd, J = 7.0 and 2.2 Hz, H-7), 7.37–7.48 (4H, m, H-3, H-5, H-6, H-5′), 7.65 (2H, d, J = 8.3 Hz, H-4″, H-6″), 8.15 (1H, dd, J = 8.2 and 1.4 Hz, H-4), 8.91–8.93 (1H, m, H-2); ^{13}C NMR (50 MHz, $CDCl_3$): δ 22.50 (C-3′), 28.59 (C-2′), 53.53 (C-1″), 68.06 (C-1′), 94.52 (C-5″), 109.12 (C-7), 119.77 (C-5), 121.47 (C-3, C-5′), 127.01 (C-6), 129.84 (C-10, C-3″, C-7″), 134.71 (C-2″), 136.42 (C-4), 138.29 (C-4″, C-6″), 140.12 (C-9), 148.05 (C-4′), 149.20 (C-2), 154.62 (C-8); HRMS (ESI) m/z: [M+H]$^+$ calcd for $C_{21}H_{19}IN_4O$, 471.0681; found, 471.0676.

4.5.2. 8-(3-(1-(4-Fluorobenzyl)-1H-1,2,3-triazol-4-yl)propoxy) quinoline (**10b**)

Yellow solid; yield 86%; m.p. 81-73 °C; IR (ATR): 1221 (C–F), 1260 and 1103 (C–O); ^{1}H NMR (400 MHz, $CDCl_3$): δ 2.34 (2H, brs, H-2′), 2.95 (2H, brs, H-3′), 4.23 (2H, brs, H-1′), 5.36 (2H, s, H-1″), 6.89–6.98 (3H, m, H-7, H-4″, H-6″), 7.10–7.16 (2H, m, H-3″, H-7″), 7.30–7.35 (4H, m, H-3, H-5, H-6, H-5′), 8.06 (1H, sl, H-4), 8.86 (1H, sl, H-2); ^{13}C NMR (50 MHz, $CDCl_3$): δ 22.28 (C-3′), 28.37 (C-2′), 53.11 (C-1″), 67.86 (C-1′), 108.80 (C-7), 115.89 (d, J = 21.6 Hz, C-4″, C-6″), 119.71 (C-5), 121.16 (C-3, C-5′), 126.74 (C-6), 129.72 (d, J = 8.2 Hz, C-3″, C-7″, C-10), 130.77 (d, J = 2.8 Hz, C-2″), 135.86 (C-4), 140.32 (C-9), 147.76 (C-4′), 149.09 (C-2), 154.63 (C-8), 162.62 (d, J = 246.3 Hz, C-5″); HRMS (ESI) m/z: [M+H]$^+$ calcd for $C_{21}H_{19}FN_4O$, 363.1621; found, 363.1616.

4.5.3. 8-(3-(1-(4-Chlorobenzyl)-1H-1,2,3-triazol-4-yl)propoxy) quinoline (**10c**)

Yellow wax; yield 81%; IR (ATR): 1260 and 1105 (C–O); ^{1}H NMR (400 MHz, $CDCl_3$): δ 2.39 (2H, brs, H-2′), 3.01 (2H, t, J = 6.8 Hz, H-3′), 4.28 (2H, brs, H-1′), 5.42 (2H, s, H-1″), 7.03–7.05 (1H, m, H-7), 7.12–7.14 (2H, m, H-3″, H-7″), 7.27–7.29 (2H, m, H-4″, H-6″), 7.36–7.44 (4H, m, H-3, H-5, H-6, H-5′), 8.13 (1H, d, J = 6.0 Hz, H-4), 8.91 (1H, brs, H-2); ^{13}C NMR (50 MHz, $CDCl_3$): δ 22.46 (C-3′), 28.52 (C-2′), 53.31 (C-1″), 68.05 (C-1′), 109.04 (C-7), 119.77 (C-5), 121.37 (C-3 or C-5′), 121.66 (C-3 or C-5′), 126.90 (C-6), 129.31 and 129.59 (C-10, C-3″, C-4″, C-6″, C-7″), 133.54 (C-5″), 134.68 (C-2″), 136.14 (C-4), 140.37 (C-9), 147.99 (C-4′), 149.24 (C-2), 154.70 (C-8); HRMS (ESI) m/z: [M+H]$^+$ calcd for $C_{21}H_{19}ClN_4O$, 379.1326 (^{35}Cl), 381.1296 (^{37}Cl); found, 379.1332 (^{35}Cl), 381.1315 (^{37}Cl).

4.5.4. 8-(3-(1-(4-Bromobenzyl)-1H-1,2,3-triazol-4-yl)propoxy) quinoline (**10d**)

Yellow oil; yield 85%; IR (ATR): 1260 and 1105 (C–O); ^{1}H NMR (400 MHz, $CDCl_3$): δ 2.38 (2H, qn, J = 6.8 Hz, H-2′), 3.01 (2H, t, J = 6.8 Hz, H-3′), 4.28 (2H, t, J = 6.8 Hz, H-1′), 5.41 (2H, s, H-1″), 7.03–7.08 (3H, m, H-7, H-3″, H-7″), 7.29–7.44 (6H, m, H-3, H-5, H-6, H-5′, H-4″, H-6″), 8.14 (1H, d, J = 8.0 Hz, H-4), 8.92 (1H, brs, H-2); ^{13}C NMR (50 MHz, $CDCl_3$): δ 22.45 (C-3′), 28.55 (C-2′), 53.35 (C-1″), 68.06 (C-1′), 109.15 (C-7), 119.74 (C-5), 121.44 (C-3 or C-5′), 121.66 (C-3 or C-5′), 122.79 (C-5″), 126.98 (C-6), 129.62 (C-10, C-3″, C-7″), 132.26 (C-4″, C-6″), 134.06 (C-2″), 136.39 (C-4), 140.04 (C-9), 147.98 (C-4′), 149.09 (C-2), 154.56 (C-8); HRMS (ESI) m/z: [M+H]$^+$ calcd for

$C_{21}H_{19}BrN_4O$, 423.0821 (^{79}Br), 425.0800 (^{81}Br); found, 423.0820 (^{79}Br), 425.0806 (^{81}Br).

4.5.5. 8-(3-(1-(4-(Trifluoromethoxy)benzyl)-1H-1,2,3-triazol-4-yl) propoxy)quinoline (**10e**)

White solid; yield 72%; m.p. 104–105 °C; IR (ATR): 1263 (C–F), 1263 and 1107 (C–O); ^1H NMR (200 MHz, $CDCl_3$): δ 2.33 (2H, qn, J = 6.8 Hz, H-2′), 2.95 (2H, t, J = 6.8 Hz, H-3′), 4.22 (2H, t, J = 6.8 Hz, H-1′), 5.39 (2H, s, H-1″), 6.95–6.98 (1H, m, H-7), 7.07–7.19 (4H, m, H-3″, H-4″, H-6″, H-7″), 7.27–7.39 (4H, m, H-3, H-5, H-6, H-5′), 8.03 (1H, d, J = 8.2 Hz, H-4), 8.85 (1H, brs, H-2); ^{13}C NMR (50 MHz, $CDCl_3$): δ 22.35 (C-3′), 28.38 (C-2′), 52.98 (C-1″), 67.88 (C-1′), 108.85 (C-7), 119.60 (C-5), 120.33 (q, J = 255.7 Hz, $\underline{C}F_3$), 121.36 and 121.51 (C-3, C-5′, C-4″, C-6″), 126.70 (C-6), 129.30 (C-10, C-3″, C-7″), 133.69 (C-2″), 135.95 (C-4), 140.21 (C-9), 147.86 (C-4′), 149.14 (C-2, C-5″), 154.54 (C-8); HRMS (ESI) m/z: $[M+H]^+$ calcd for $C_{22}H_{19}F_3N_4O_2$, 429.1538; found, 429.1534.

4.5.6. 8-(3-(1-(3,4-Difluorobenzyl)-1H-1,2,3-triazol-4-yl)propoxy) quinoline (**10f**)

Beige solid; yield 89%; m.p. 90–91 °C; IR (ATR): 1210 (C–F), 1259 and 1103 (C–O); ^1H NMR (400 MHz, $CDCl_3$): δ 2.40 (2H, qn, J = 7.2 Hz, H-2′), 3.02 (2H, t, J = 7.2 Hz, H-3′), 4.29 (2H, t, J = 7.2 Hz, H-1′), 5.41 (2H, s, H-1″), 6.93–6.95 (1H, m, H-7), 7.02–7.11 (3H, m, H-3″, H-6″, H-7″), 7.37–7.45 (4H, m, H-3, H-5, H-6, H-5′), 8.14 (1H, d, J = 8.4 Hz, H-4), 8.93 (1H, brs, H-2); ^{13}C NMR (50 MHz, $CDCl_3$): δ 22.01 (C-3′), 28.16 (C-2′), 52.33 (C-1″), 67.52 (C-1′), 108.59 (C-7), 116.65 (d, J = 17.8 Hz, C-3″), 117.46 (d, J = 17.4 Hz, C-6″), 119.33 (C-5), 121.27 (C-3, C-5′), 123.78 (dd, J = 6.2 and 3.6 Hz, C-7″), 126.47 (C-6), 129.14 (C-10), 131.42–131.60 (m, C-2″), 135.74 (C-4), 139.79 (C-9), 147.55 (C-4′), 148.75 (C-2), 147.36–152.48 (m, C-4″ and C-5″), 154.19 (C-8); HRMS (ESI) m/z: $[M+H]^+$ calcd for $C_{21}H_{18}F_2N_4O$, 381.1527; found, 381.1522.

4.5.7. 8-(3-(1-(2,4,6-Trichlorobenzyl)-1H-1,2,3-triazol-4-yl)propoxy) quinoline (**10g**)

Green–white solid; yield 73%; m.p. 86–88 °C; IR (ATR): 1073 (C–Cl), 1260 and 1106 (C–O); ^1H NMR (200 MHz, $CDCl_3$): δ 2.28–2.35 (2H, m, H-2′), 2.93 (2H, t, J = 6.4 Hz, H-3′), 4.18 (2H, t, J = 6.4 Hz, H-1′), 5.63 (2H, s, H-1″), 6.93–6.96 (1H, m, H-7), 7.25–7.34 (6H, m, H-3, H-5, H-6, H-5′, H-4″, H-6″), 8.04 (1H, d, J = 8.0 Hz, H-4), 8.85 (1H, brs, H-2); ^{13}C NMR (50 MHz, $CDCl_3$): δ 22.05 (C-3′), 28.25 (C-2′), 48.20 (C-1″), 67.60 (C-1′), 108.74 (C-7), 119.46 (C-5), 121.40 (C-3, C-5′), 126.61 (C-6), 128.65 (C-4″, C-6″), 128.83 (C-5″ or C-10), 129.32 (C-10 or C-5″), 135.86 (C-2″, C-4), 137.02 (C-3″, C-7″), 140.12 (C-9), 147.00 (C-4′), 149.09 (C-2), 154.46 (C-8); HRMS (ESI) m/z: $[M+H]^+$ calcd for $C_{21}H_{17}Cl_3N_4O$, 447.0546 (3× ^{35}Cl), 449.0517 (2× ^{35}Cl + 1× ^{37}Cl), 451.0487 (2× ^{37}Cl + 1× ^{35}Cl); found, 447.0541 (3× ^{35}Cl), 449.0509 (2× ^{35}Cl + 1× ^{37}Cl), 451.0499 (2× ^{37}Cl + 1× ^{35}Cl).

4.5.8. 8-(3-(1-(5-Bromo-2-chlorobenzyl)-1H-1,2,3-triazol-4-yl) propoxy)quinoline (**10h**)

Yellow oil; yield 94%; IR (ATR): 1259 and 1105 (C–O); ^1H NMR (200 MHz, $CDCl_3$): δ 2.42 (2H, qn, J = 6.8 Hz, H-2′), 3.05 (2H, t, J = 6.8 Hz, H-3′), 4.30 (2H, t, J = 6.8 Hz, H-1′), 5.55 (2H, s, H-1″), 7.04–7.07 (1H, m, H-7), 7.20–7.29 (2H, m, H-5″, H-6″), 7.36–7.49 (4H, m, H-3, H-5, H-6, H-5′), 7.49 (1H, s, H-3″), 8.14 (1H, d, J = 8.2 Hz, H-4), 8.93 (1H, brs, H-2); ^{13}C NMR (50 MHz, $CDCl_3$): δ 22.48 (C-3′), 28.54 (C-2′), 50.83 (C-1″), 68.02 (C-1′), 109.09 (C-7), 119.72 (C-5), 121.22 (C-3 or C-5′), 121.67 (C-3 or C-5′), 121.89 (C-4″), 126.99 (C-6), 129.62 (C-10), 131.28 (C-5″), 132.24 (C-7″), 132.84 (C-3″ or C-6″), 133.15 (C-3″ or C-6″), 134.78 (C-2″), 136.34 (C-4), 140.08 (C-9), 147.95 (C-4′), 149.15 (C-2), 154.57 (C-8); HRMS (ESI) m/z: $[M+H]^+$ calcd for $C_{21}H_{18}BrClN_4O$, 457.0431 (^{79}Br and ^{35}Cl), 459.0410 (^{81}Br or ^{37}Cl), 461.0381 (^{81}Br and ^{37}Cl); found, 457.0428 (^{79}Br and ^{35}Cl), 459.0408 (^{81}Br or ^{37}Cl), 461.0382 (^{81}Br and ^{37}Cl).

4.5.9. 8-(3-(1-Benzyl-1H-1,2,3-triazol-4-yl)propoxy)quinoline (**10i**)

Yellow solid; yield 92%; m.p. 63–65 °C; IR (ATR): 1258 and 1105 (C–O); ^1H NMR (200 MHz, $CDCl_3$): δ 2.34–2.40 (2H, m, H-2′), 2.98 (2H, t, J = 6.4 Hz, H-3′), 4.26 (2H, t, J = 6.4 Hz, H-1′), 5.43 (2H, s, H-1″), 6.99–7.04 (1H, m, H-7), 7.16–7.24 (2H, m, H-3″, H-7″), 7.28–7.43 (7H, m, H-3, H-5, H-6, H-5′, H-4″, H-5″, H-6″), 8.09 (1H, d, J = 8.0 Hz, H-4), 8.90 (1H, brs, H-2); ^{13}C NMR (50 MHz, $CDCl_3$): δ 22.19 (C-3′), 28.34 (C-2′), 53.75 (C-1″), 67.79 (C-1′), 108.80 (C-7), 119.47 (C-5), 121.17 (C-3, C-5′), 126.69 (C-6, C-5″), 127.72 (C-3″, C-7″), 128.37 and 128.83 (C-10, C-4″, C-6″), 134.79 (C-2″), 135.96 (C-4), 139.90 (C-9), 147.47 (C-4′), 148.83 (C-2), 154.39 (C-8); HRMS (ESI) m/z: $[M+H]^+$ calcd for $C_{21}H_{20}N_4O$, 345.1715; found, 345.1711.

4.5.10. 8-(3-(1-(3-(Pyridin-3-yl)propyl)-1H-1,2,3-triazol-4-yl) propoxy)quinoline (**15**)

Yellow solid; yield 67%; m.p. 82–83 °C; IR (ATR): 1261 and 1105 (C–O); ^1H NMR (200 MHz, $CDCl_3$): δ 2.19 (2H, qn, J = 7.0 Hz, H-2′), 2.42 (2H, qn, J = 7.0 Hz, H-2″), 2.69 (2H, t, J = 7.0 Hz, H-3′), 3.04 (2H, t, J = 7.0 Hz, H-3″), 4.32 (4H, t, J = 7.0 Hz, H-1′, H-1″), 7.07 (1H, dd, J = 7.2 and 1.8 Hz, H-7), 7.26–7.51 (6H, m, H-3, H-5, H-6, H-5′, H-8″, H-9″), 8.12–8.16 (1H, m, H-4), 8.56 (2H, ls, H-5″, H-7″), 8.95 (1H, ls, H-2); ^{13}C NMR (50 MHz, $CDCl_3$): δ 22.44 (C-3′), 28.56 (C-2′), 29.79 (C-2″), 31.42 (C-3″), 49.21 (C-1″), 68.05 (C-1′), 108.98 (C-7), 119.69 (C-5), 121.37 (C-3, C-5′), 126.86 (C-6, C-8″), 129.60 (C-10), 135.96 and 136.14 (C-4, C-4″, C-9″), 140.21 (C-9), 147.47 (C-4′, C-7″), 149.66 (C-2, C-5″), 154.61 (C-8); HRMS (ESI) m/z: $[M+H]^+$ calcd for $C_{22}H_{23}N_5O$, 374.1981; found, 374.1983.

4.5.11. 8-(3-(1-1,2:3,4-di-O-isopropylidene-6-α-D-galactopyranosyl-1H-1,2,3-triazol-4-yl) propoxy)quinoline (**16**)

White solid; yield 72%; m.p. 123–124 °C; IR (ATR): 1255, 1103 and 1078 (C–O); ^1H NMR (200 MHz, $CDCl_3$): δ 1.28, 1.34, 1.37 and 1.49 (s, 12H, 4× $C\underline{H}_3$), 2.39–2.46 (2H, m, H-2′), 3.02 (2H, t, J = 7.2 Hz, H-3′), 4.15–4.18 (2H, m, H-4″, H-5″), 4.27–4.36 (3H, m, H-1′, H-2″), 4.45 (1H, d, J = 8.0 Hz, H-6″), 4.55–4.64 (2H, m, H-3″, H-6″), 5.49 (1H, d, J = 4.8 Hz, H-1″), 7.07 (1H, dd, J = 7.2 and 1.6 Hz, H-7), 7.38–7.44 (3H, m, H-3, H-5, H-6), 7.57 (1H, s, H-5′), 8.12 (1H, dd, J = 4.2 and 1.6 Hz, H-4), 8.95 (1H, dd, J = 8.2 and 1.6 Hz, H-2); ^{13}C NMR (50 MHz, $CDCl_3$): δ 22.46 (C-3′), 24.50, 24.97, 26.02 and 26.07 (4× $C\underline{H}_3$), 28.66 (C-2′), 50.41 (C-6″), 67.37 (C-5″), 68.09 (C-1′), 70.41, 70.82 and 71.23 (C-2″, C-3″, C-4″), 96.31 (C-1″), 108.96 (C-7), 109.09 and 109.89 (2× $\underline{C}(CH_3)_2$), 119.63 (C-5), 121.61 (C-3), 122.53 (C-5′), 126.80 (C-6), 129.57 (C-10), 135.98 (C-4), 140.49 (C-9), 147.00 (C-4′), 149.37 (C-2), 154.83 (C-8); HRMS (ESI) m/z: $[M+H]^+$ calcd for $C_{26}H_{32}N_4O_6$, 497.2400; found, 497.2398.

4.5.12. 3,4-Difluorobenzyl 2-(4-(3-(quinolin-8-yloxy)propyl)-1H-1,2,3-triazol-1-yl)acetate (**17**)

White solid; yield 80%; m.p. 104–105 °C; IR (ATR): 1754 (C=O), 1261 and 1108 (C–O); ^1H NMR (200 MHz, $CDCl_3$): δ 2.37–2.44 (2H, m, H-2′), 3.02 (2H, t, J = 6.8 Hz, H-3′), 4.30 (2H, t, J = 6.8 Hz, H-1′), 5.09 (2H, s, H-6′), 5.17 (2H, s, H-1″), 7.03–7.16 (4H, m, H-7, H-3″, H-6″, H-7″), 7.39–7.61 (3H, m, H-3, H-5, H-6), 7.61 (1H, s, H-5′), 8.09–8.13 (1H, m, H-4), 8.91 (1H, brs, H-2); ^{13}C NMR (50 MHz, $CDCl_3$): δ 22.41 (C-3′), 28.44 (C-2′), 50.68 (C-6′), 66.41 (C-1″), 67.99 (C-1′), 108.99 (C-7), 117.59 (d, J = 17.4 Hz, C-3″, C-6″), 119.65 (C-5), 121.57 (C-3), 122.82 (C-5′), 124.76 (dd, J = 6.0 and 3.9 Hz, C-7″), 126.82 (C-6), 129.52 (C-10), 131.53–131.72 (m, C-2″), 136.09 (C-4), 140.19 (C-9), 147.80 (C-4′) 147.56–152.88 (m, C-4″, C-5″), 149.12 (C-2), 154.57 (C-8), 166.26 (C-7′); HRMS (ESI) m/z: $[M+H]^+$ calcd for $C_{23}H_{20}F_2N_4O_3$, 439.1582; found, 439.1584.

4.6. Antiproliferative assay

The obtained 1,2,3-triazoles were each evaluated for their *in vitro* antiproliferative activity against HaCat cells (human keratinocytes), a normal human normal cell line, as well as seven human cancer cell lines: U251 (glioma, CNS), MCF-7 (breast), NCI-ADR/RES (ovarian, multidrug resistant), 786-0 (kidney), NCI-H460 (lung, non-small cell), PC-3 (prostate), and OVCAR-03 (ovarian). The cancer cell lines were kindly provided by the United States National Cancer Institute (Frederick, MA, USA), while the HaCat cell line was kindly donated by Dr. Ricardo Della Coletta (FOP, UNICAMP). Stock cultures were grown in 5 mL of RPMI-1640 (Gibco BRL) supplemented with 5% fetal bovine serum (Gibco BRL). A penicillin (1000 U mL^{-1}):streptomycin (1000 μg mL^{-1}) mixture (1 mL L^{-1} RPMI) was added to the experimental cultures.

Cells were placed in 96-well plates (100 μL cells/well) and were exposed to different concentrations of compounds **10a**–**i**, **15**, **16**, and **17** (0.25, 2.5, 25, and 250 μg mL^{-1}) in DMSO/RPMI (0.1% v/v) at 37 °C and 5% CO_2 for 48 h. The final DMSO concentration did not affect cell viability. Next, the cells were fixed with aqueous solution of trichloroacetic acid (50%, v/v) and cell proliferation was measured by performing spectrometry (540 nm) on the cellular protein content using a sulforhodamine B assay [45]. All experiments were performed in triplicate. Doxorubicin (0.025–25 μg mL^{-1}) was used as a positive control. Measurements were obtained at three time points for both the compound-free (C) and the tested (T) cells: time zero (T_o), the beginning of incubation, and 48 h post-incubation. Cell proliferation was calculated according to the equation: $100 \times [(T - T_o)/C - T_o]$. A cytostatic effect was observed when $T \geq T_o$, whereas a cytocidal effect occurred when $T < T_o$. Based on the concentration–response curve for each cell line, a GI_{50} value (the concentration that caused 50% cell growth inhibition or a cytostatic effect) was determined by non-linear regression analysis using Origin 8.0® software (OriginLab Corporation). Furthermore, a mean graph midpoint (MG MID, mean of log GI_{50}) was calculated for the GI_{50} values obtained for each sample, using MS Excel software. MG MID displays an averaged activity parameter over all cell lines. The selectivity index (SI) was determined according to the equation: IS = HaCat cell GI_{50}/cancer cell GI_{50}. SI values greater than two were considered significant [49,50].

4.7. Physico-chemical parameter calculations

Physicochemical parameters were calculated using the software provided by Molinspiration Cheminformatics [42]. The following molecular attributes analyzed: n-octanol/water partition coefficient (cLog*P*), the numbers of HBD and HBA, molecular weights of the compounds (MW), nRotb, and PSA. The numbers of HBDs and HBAs were calculated as described by Lipinski and co-workers [37]. The PSA of each molecule was calculated by the aforementioned software using the method described by Ertl and co-authors [37,42].

4.8. SAR studies and theoretical calculations

The calculations were performed using the Spartan Pro [51] and Gaussian 09 [52] packages. Initially, a systematic conformational analysis was made using 30° rotations in all single bonds. Each confirmation was fully optimized by means of two consecutive methods: semiempirical PM3tm and density functional theory (DFT). For each of the calculation methods, the conjugate gradient and quasi-Newton–Raphson algorithms were used for geometry optimization until a gradient of 10^{-4} kcal mol^{-1} $Å^{-1}$ was obtained. The final geometries were obtained by DFT using the Becke–Perdew perturbative model with the numerical polarization basis set DN*. The final structures were again optimized until a gradient of 10^{-8} kcal mol^{-1} $Å^{-1}$ was obtained. No imaginary frequencies were found for the optimized geometries. These optimized geometries were used in all subsequent calculations. MP2 single-point energy calculations were computed using the 6-311G(d,p) basis set. The orbital energies from these methods were fitted to a linear model with experimental antiproliferative activity values. The determination coefficients and other statistical parameters were analyzed using the Molegro Virtual Docker (MVD) [53]. The molecular obritals figures were generated by the Gaussian View 2.1 package72 using a contour value of 0.020. In order to clarify the binding mode between ligand and enzyme, docking calculations were performed for the studied compounds in the active site of α-glucosidase. The crystal structure of α-glucosidase was obtained from the Protein Data Bank (PDB code: 3L4Y) [54]. The docking calculation of the ligands inside α-glucosidase active site was performed using MVD software [53]. This program is able to predict the most likely conformation by which a given ligand will bind to a macromolecule.

Conflict of interest

The authors have declared no conflict of interest.

Acknowledgments

This research was supported by grants from CNPq (Conselho Nacional de Desenvolvimento Científico e Tecnológico), CAPES (Coordenação de Aperfeiçoamento de Pessoal de Nível Superior), FAPEMIG (Fundação de Amparo à Pesquisa do estado de Minas Gerais) and PRPq (Pró-Reitoria de Pesquisa da Universidade Federal de Minas Gerais).

Appendix A. Supplementary data

Supplementary data related to this article can be found at http://dx.doi.org/10.1016/j.ejmech.2014.07.061.

References

[1] A. Jemal, F. Bray, M.M. Center, J. Ferlay, E. Ward, D. Forman, Global cancer statistics, CA Cancer J. Clin. 61 (2011) 69–90.
[2] G. Colombano, C. Travelli, U. Galli, A. Caldarelli, M.G. Chini, P.L. Canonico, G. Sorba, G. Bifulco, G.C. Tron, A.A. Genazzani, A novel potent nicotinamide phosphoribosyltransferase inhibitor synthesized via click chemistry, J. Med. Chem. 53 (2010) 616–623.
[3] V. Spanò, A. Montalbano, A. Carbone, B. Parrino, P. Diana, G. Cirrincione, I. Castagliuolo, P. Brun, O.-G. Issinger, S. Tisi, I. Primac, D. Vedaldi, A. Salvador, P. Barraja, Synthesis of a new class of pyrrolo[3,4-*h*]quinazolines with antimitotic activity, Eur. J. Med. Chem. 74 (2014) 340–357.
[4] R. Dua, S. Shrivastava, S.K. Sonwane, S.K. Shrivastava, Pharmacological significance of synthetic heterocycles scaffold: a review, Adv. Biol. Res. 5 (2011) 120–144.
[5] P. Diana, A. Carbone, P. Barraja, A. Montalbano, B. Parrino, A. Lopergolo, M. Pennati, N. Zaffaroni, G. Cirrincione, Synthesis and antitumor activity of 3-(2-phenyl-1,3-thiazol-4-yl)-1*H*-indoles and 3-(2-phenyl-1,3-thiazol-4-yl)-1*H*-7-azaindoles, ChemMedChem 6 (2011) 1300–1309.
[6] K.D. Thomas, A.V. Adhikari, N.S. Shetty, Design, synthesis and antimicrobial activities of some new quinoline derivatives carrying 1,2,3-triazole moiety, Eur. J. Med. Chem. 45 (2010) 3803–3810.
[7] P. Barraja, P. Diana, A. Montalbano, A. Carbone, G. Viola, G. Basso, A. Salvador, D. Vedaldi, F. Dall'Acqua, G. Cirrincione, Pyrrolo[3,4-*h*]quinolinones a new class of photochemotherapeutic agents, Bioorg. Med. Chem. 19 (2011) 2326–2341.
[8] K. Kaur, M. Jain, R.P. Reddy, R. Jain, Quinolines and structurally related heterocycles as antimalarials, Eur. J. Med. Chem. 45 (2010) 3245–3264.
[9] V. Moret, Y. Laras, T. Cresteil, G. Aubert, D.Q. Ping, C. Di, M.B. Requin, C. B'eclin, V. Peyrot, D. Allegro, A. Rolland, F.D. Angelis, E. Gatti, P. Pierre, L. Pasquini, E. Petrucci, U. Testa, J.L. Kraus, Discovery of a new family of bis-8-hydroxyquinoline substituted benzylamines with pro-apoptotic activity in cancer cells: synthesis, structure-activity relationship, and action mechanism studies, Eur. J. Med. Chem. 44 (2009) 558–567.

[10] A.M. Rashad, W.A. El-Sayed, A.M. Mohamed, M.M. Ali, Synthesis of new quinoline derivatives as inhibitors of human tumor cells growth, Arch. Pharm. Chem. Life Sci. 343 (2010) 440–448.
[11] R.K. Arafa, G.H. Hegazy, G.A. Piazza, A.H. Abadi, Synthesis and in vitro anti-proliferative effect of novel quinolone-based potential anticancer agents, Eur. J. Med. Chem. 63 (2013) 826–832.
[12] R. Musiol, J. Jampilek, V. Buchta, H. Niedbala, B. Podeszwa, A. Palka, K. Majerz-Maniecka, B. Oleksyn, J. Polanski, Antifungal properties of new series of quinoline derivatives, Bioorg. Med. Chem. 14 (2006) 3592–3598.
[13] J. Sharma, S. Hussain, M. Amir, Synthesis and study of some newer analogues of quinolin-8-ol as potent antimicrobial agents, E J. Chem. 5 (2008) 1008–1014.
[14] R. Musiol, J. Jampilek, J.E. Nycz, M. Pesko, J. Carroll, K. Kralova, M. Vesjova, J. O'Mahony, A. Coffey, A. Mrozek, J. Polansky, Investigating the activity spectrum for ring-substituted 8-hydroxyquinolines, Molecules 15 (2010) 288–304.
[15] P.A. Enquist, Å. Gylfe, U. Hagglund, P. Lindström, H.N. Scherman, C. Sundin, M. Elofsson, Derivatives of 8-hydroxyquinoline-antibacterial agents that target intra- and extracellular gram-negative pathogens, Bioorg. Med. Chem. Lett. 22 (2012) 3550–3553.
[16] S.S. Chhajed, P. Manicha, V.A. Bastikar, H. Animeshchandra, V.N. Ingle, C.D. Upasani, S.S. Wazalwar, Synthesis and molecular modeling studies of 3-chloro-4-substituted-1-(8-hydroxy-quinolin-5-yl)-azetidin-2-ones as novel anti-filarial agents, Bioorg. Med. Chem. Lett. 20 (2010) 3640–3644.
[17] J. Polanski, H. Niedbala, R. Musiol, B. Podeszwa, D. Tabak, A. Palka, A. Mencel, J.-F. Finster, M.L.B. Mouscadet, 5-Hydroxy-6-quinaldic acid as a novel molecular scaffold for HIV-1 integrase inhibitors, Lett. Drug Des. Discov. 3 (2006) 175–178.
[18] S.G. Agalave, S.R. Maujan, V.S. Pore, Click chemistry: 1,2,3-triazoles as pharmacophores, Chem. Asian J. 6 (2011) 2696–2718.
[19] M. Meldal, C.W. Tornøe, Cu-catalyzed azide-alkyne cycloaddition, Chem. Rev. 108 (2008) 2952–3015.
[20] M.J. Giffin, H. Heaslet, A. Brik, Y.-C. Lin, G. Cauvi, C.-H. Wong, D.E. McRee, J.H. Elder, C.D. Stout, B.E. Torbett, A copper(I)-catalyzed 1,2,3-triazole azide-alkyne click compound is a potent inhibitor of a multidrug-resistant HIV-1 protease variant, J. Med. Chem. 51 (2008) 6263–6270.
[21] E.N. Silva Júnior, M.A.B.F. Moura, A.V. Pinto, M.C.F.R. Pinto, M.C.B.V. Souza, A.J. Araújo, C. Pessoa, L.V.C. Lotufo, R.C. Montenegro, M.O. Moraes, V.F. Ferreira, O.F. Goulart, Cytotoxic, trypanocidal activities and physicochemical parameters of *nor*-β-lapachone-based 1,2,3-triazoles, J. Braz. Chem. Soc. 20 (2009) 635–643.
[22] J.V. Anjos, R.A.W. Neves Filho, S.C. Nascimento, R.M. Srivastava, S.J. Melo, D. Sinou, Synthesis and cytotoxic profile of glycosyl–triazole linked to 1,2,4-oxadiazole moiety at C-5 through a straight-chain carbon and oxygen atoms, Eur. J. Med. Chem. 44 (2009) 3571–3576.
[23] A. Kamal, N. Shankaraiah, V. Devaiah, K.L. Reddy, A. Juvekar, S. Sen, N. Kurian, S. Zingde, Synthesis of 1,2,3-triazole-linked pyrrolobenzodiazepine conjugates employing 'click' chemistry: DNA-binding affinity and anticancer activity, Bioorg. Med. Chem. Lett. 18 (2008) 1468–1473.
[24] H. Gallardo, G. Conte, F. Bryk, M.C.S. Lourenço, M.S. Costa, V.F. Ferreira, Synthesis and evaluation of 1-alkyl-4-phenyl-[1,2,3]-triazole derivatives as antimycobacterial agent, J. Braz. Chem. Soc. 18 (2007) 1285–1291.
[25] N. Boechat, V.F. Ferreira, S.B. Ferreira, M.L.G. Ferreira, F.C. Silva, M.M. Bastos, M.S. Costa, M.C.S. Lourenço, A.C. Pinto, A.U. Krettli, A.C. Aguiar, B.B. Teixeira, N.V. Silva, P.R.C. Martins, F.A.F.M. Bezerra, A.L.S. Camilo, G.P. Silva, C.C.P. Costa, Novel 1,2,3-triazole derivatives for use against *Mycobacterium tuberculosis* H37Rv (ATCC 27294) strain, J. Med. Chem. 54 (2011) 5988–5999.
[26] V.S. Pore, N.G. Aher, M. Kumar, P.K. Shukla, Design and synthesis of fluconazole/bile acid conjugate using click reaction, Tetrahedron 62 (2006) 11178–11186.
[27] N.G. Aher, V.S. Pore, N.N. Mishra, A. Kumar, P.K. Shukla, A. Sharma, M.K. Bhat, Synthesis and antifungal activity of 1,2,3-triazole containing fluconazole analogues, Bioorg. Med. Chem. Lett. 19 (2009) 759–763.
[28] E.M. Guantai, K. Ncokazi, T.J. Egan, J. Gut, P.J. Rosenthal, P.J. Smith, K. Chibale, Design, synthesis and in vitro antimalarial evaluation of triazole-linked chalcone and dienone hybrid compounds, Bioorg. Med. Chem. 18 (2010) 8243–8256.
[29] I. Carvalho, P. Andrade, V.L. Campo, P.M.M. Guedes, R. Sesti-Costa, J.S. Silva, S. Schenkman, S. Dedola, L. Hill, M. Rejzek, S.A. Nepogodiev, R.A. Field, 'Click chemistry' synthesis of a library of 1,2,3-triazole-substituted galactose derivatives and their evaluation against *Trypanosoma cruzi* and its cell surface trans-sialidase, Bioorg. Med. Chem. 18 (2010) 2412–2427.
[30] E.N. Silva Jr., R.F.S.M. Barreto, M.C.F.R. Pinto, R.S.F. Silva, D.V. Teixeira, M.C.B.V. Souza, C.A. Simone, S.L. Castro, V.F. Ferreira, A.V. Pinto, Naphthoquinoidal [1,2,3]-triazole, a new structural moiety active against *Trypanosoma cruzi*, Eur. J. Med. Chem. 43 (2008) 1774–1780.
[31] F. Pisaneschi, Q.-D. Nguyen, E. Shamsaei, M. Glaser, E. Robins, M. Kaliszczak, G. Smith, A.C. Spivey, E.O. Aboagye, Development of a new epidermal growth factor receptor positron emission tomography imaging agent based on the 3-cyanoquinoline core: synthesis and biological evaluation, Bioorg. Med. Chem. 18 (2010) 6634–6645.
[32] K.K. Kumar, S.P. Seenivasan, V. Kumar, T.M. Das, Synthesis of quinolone coupled [1,2,3]-triazoles as a promising class of anti-tuberculosis agents, Carbohydr. Res. 346 (2011) 2084–2090.
[33] Y.-M. Zhang, Y. Chen, Z.-Q. Li, N. Li, Y. Liu, Quinolinotriazole-β-cyclodextrin and its adamantanecarboxylic acid complex as efficient water-soluble fluorescent Cd^{2+} sensors, Bioorg. Med. Chem. 18 (2010) 1415–1420.
[34] Y. Yao, Z. Sun, Z. Zou, H. Li, Quinolino-triazole linked gold nanoparticles as sensitive 'turn-on' fluorescent Cd^{2+} probes, Nanotechnology 22 (2011) 435502–435506.
[35] G.L. Bundy, C.H. Lin, J.C. Sih, The synthesis of 2,3-dinorprostacyclin metabolites- a new approach to spirolactone hemiacetals, Tetrahedron 37 (1981) 4419–4429.
[36] S.B. Ferreira, A.C.R. Sodero, M.F.C. Cardoso, E.S. Lima, C.R. Kaiser, F.P. Silva Jr., V.F. Ferreira, Synthesis, biological activity, and molecular modeling studies of 1*H*-1,2,3-triazole derivatives of carbohydrates as α-glucosidases inhibitors, J. Med. Chem. 53 (2010) 2364–2375.
[37] C.A. Lipinski, F. Lombardo, B.W. Dominy, P.J. Feeney, Experimental and computational approaches to estimate solubility and permeability in drug discovery and developments settings, Adv. Drug Deliv. Rev. 23 (1997) 3–25.
[38] C.A. Lipinski, Lead- and drug-like compounds: the rule-of-five revolutions, Drug Discov. Today Technol. 1 (2004) 337–341.
[39] D.F. Veber, S.R. Johnson, H.-Y. Cheng, B.R. Smith, K.W. Ward, K.D. Kopple, Molecular properties that influence the oral bioavailability of drug candidates, J. Med. Chem. 45 (2002) 2615–2623.
[40] Software available free of charge at http://www.molinspiration.com. Bratislava, Slovak Republic.
[41] A.K. Ghose, G.M. Crippen, Atomic physicochemical parameters for three-dimensional structure-directed quantitative structure-activity relationships I. partition coefficients as a measure of hydrophobicity, J. Comput. Chem. 7 (1986) 565–577.
[42] D.E. Clark, S.D. Pickett, Computational methods for the prediction of 'drug-likeness', Drug Discov. Today 5 (2000) 49–58.
[43] H.J. Kim, H.J. Cho, H. Kim, M.I. El-Gamal, C.-H. Oh, S.H. Lee, T. Sim, J.-M. Hah, K.H. Yoo, New diarylureas and diarylamides possessing acet(benz)amidophenyl scaffold: design, synthesis, and antiproliferative activity against melanoma cell line, Bioorg. Med. Chem. Lett. 22 (2012) 3269–3273.
[44] A.J. Hopfinger, S. Wang, J.S. Tokarski, B. Jin, M. Albuquerque, P.J. Madhav, C. Duraiswami, Construction of 3D-QSAR models using the 4D-QSAR analysis formalism, J. Am. Chem. Soc. 119 (1997) 10509–105015.
[45] C. Vikas, Externally predictive quantitative modeling of supercooled liquid vapor pressure of polychlorinated-naphthalenes through electron-correlation base quantum-mechanical descriptors, Chemosphere 95 (2014) 448–454.
[46] Y. Chinthala, A.K. Domatti, A. Sarfaraz, S.P. Singh, N.K. Arigari, N. Gupta, S.K.V.N. Satya, J.K. Kumar, F. Khan, A.K. Tiwari, G. Paramjit, Synthesis, biological evaluation and molecular modeling studies of some novel thiazolidinediones with triazole ring, Eur. J. Med. Chem. 70 (2013) 308–314.
[47] T.M. Wrodnigg, A.J. Steiner, B.J. Ueberbacher, Natural and synthetic iminosugars as carbohydrate processing enzyme inhibitors for cancer therapy, Anticancer Agents Med. Chem. 8 (2008) 77–85.
[48] Y. Zhao, Y. Zhou, K.M. O' Boyle, P.V. Murphy, Biological study of the angiogenesis inhibitor *N*-(8-(3-ethynylphenoxy)octyl-1-deoxynojirimycin, Chem. Biol. Drug Des. 75 (2010) 570–577.
[49] A. Monks, D. Scudiero, P. Skehan, R. Shoemaker, K. Paull, D. Vistica, C. Hose, J. Langley, P. Cronise, A. VaigroWolff, Feasibility of a high-flux anticancer drug screen using a diverse panel of cultured human tumor cell lines, J. Natl. Cancer Inst. 83 (1991) 757–766.
[50] M. Suffness, J.M. Pezzuto, Assays related to cancer drug discovery, in: Hostettmann (Ed.), Methods in Plant Biochemistry: Assays for Bioactivity, sixth ed., Academic Press, London, 1990.
[51] W.J. Hehre, B.J. Deppmeier, P.E. Klunzinger, PC SPARTAN Pro, Wavefunction Inc., Irvine, California, 1999.
[52] M.J. Frisch, G.W. Trucks, H.B. Schlegel, G.E. Scuseria, M.A. Robb, J.R. Cheeseman, G. Scalmani, V. Barone, B. Mennucci, G.A. Petersson, H. Nakatsuji, M. Caricato, X. Li, H.P. Hratchian, A.F. Izmaylov, J. Bloino, G. Zheng, J.L. Sonnenberg, M. Hada, M. Ehara, K. Toyota, R. Fukuda, J. Hasegawa, M. Ishida, T. Nakajima, Y. Honda, O. Kitao, H. Nakai, T. Vreven, J.A. Montgomery Jr., J.E. Peralta, F. Ogliaro, M. Bearpark, J.J. Heyd, E. Brothers, K.N. Kudin, V.N. Staroverov, R. Kobayashi, J. Normand, K. Raghavachari, A. Rendell, J.C. Burant, S.S. Iyengar, J. Tomasi, M. Cossi, N. Rega, J.M. Millam, M. Klene, J.E. Knox, J.B. Cross, V. Bakken, C. Adamo, J. Jaramillo, R. Gomperts, R.E. Stratmann, O. Yazyev, A.J. Austin, R. Cammi, C. Pomelli, J.W. Ochterski, R.L. Martin, K. Morokuma, V.G. Zakrzewski, G.A. Voth, P. Salvador, J.J. Dannenberg, S. Dapprich, A.D. Daniels, Ö. Farkas, J.B. Foresman, J.V. Ortiz, J. Cioslowski, D.J. Fox, Gaussian 09, Revision D.01, Gaussian, Inc., Wallingford CT, 2009.
[53] R. Thomsen, M.H. Christensen, MolDock: a new technique for high-accuracy molecular docking, J. Med. Chem. 49 (2006) 3315–3354.
[54] L. Sim, K. Jayakanthan, S. Mohan, R. Nasi, B.D. Johnston, B.M. Pinto, D.R. Rose, New glucosidase inhibitors from an ayurvedic herbal treatment for type 2 diabetes: structures and inhibition of human intestinal maltase-glucoamylase with compounds from *Salacia reticulate*, Biochemistry 49 (2010) 443–451.